Assessment of debris flow susceptibility using bivariate and multivariate statistical analyses and verification based on catastrophic events from 2014 in the Krivánska Fatra Mountains, Slovakia

Juraj Holec[1], Martin Bednarik[2], Pavel Liščák[3], Andrej Žilka[3] & Ladislav Vitovič[1]

[1]Comenius University in Bratislava, Faculty of Natural Sciences, Department of Physical Geography and Geoecology, Ilkovičova 6, SK-842 15, Bratislava, Slovakia; juraj.holec@uniba.sk, vitovic2@uniba.sk
[2]Comenius University in Bratislava, Faculty of Natural Sciences, Department of Engineering Geology, Ilkovičova 6, SK-842 15 Bratislava, Slovakia; mbednarik@fns.uniba.sk
[3]State Geological Institute of Dionýz Štúr, Mlynská dolina 1, SK-817 04 Bratislava, Slovakia; pavel.liscak@geology.sk, andrej.zilka@geology.sk

AGEOS

Abstract: The presented study shows using of bivariate and multivariate statistical analyses in mountain area of the Krivánska Fatra Mountains affected by debris flows. Three generations of data were studied in order to assess the debris flows in the area, from these two main periods of debris flows were taken into the analysis: the debris flows from 1950s to 1970s and catastrophic debris flows from July 2014. Various input data were used in the statistical analyses: elevation, slope angle, plan curvature, topographic wetness index, flow accumulation, lithology, and land cover. Two main evaluations were made: first using the older debris flow data and second using debris flow data from the both periods. Receiver operating characteristic analysis was performed in order to assess the reliability of the models with the area under curve more than 95 % for both evaluations and more than 85 % for the first evaluation checked by both periods of debris flows in case of multivariate analysis, respectively almost 83 % and 80 % in case of bivariate analysis. The comparison with existing avalanche tracks was performed as well and shows satisfactory results. The tracks of debris flows from July 2014 show the extraordinariness of the event in comparison with older debris flows. Experimental assessment of natural hazard was performed using the map of difference between the two susceptibility maps in order to find out the areas of possible high magnitude low frequency events.

Key words: Krivánska Fatra Mts., debris flow, susceptibility map, multivariate analysis, bivariate analysis, validation processes

1. INTRODUCTION

The study of natural hazards has become an important topic in recent decades (Smith & Petley, 2009). Due to climate change and population growth, the impact of natural hazards will increase (Alexander, 2004). Among these natural hazards, debris flows play an important role mainly in mountain areas. A debris flow is typically a sudden and torrential flow of a mixture of water, mud, debris, and boulders (Takahashi, 2014). It is physically important that the material flow as a continuous fluid driven by gravity with extreme mobility due to the spaces between particles filled by water (Takahashi, 2014). Debris flows are rapid mass movements, which can cause casualties, injury as well as extensive damage to property and infrastructure especially in the Alpine areas (Carrara et al., 2008; Cama et al., 2014). Because of their velocity, they are among the most hazardous mass movements (Meyer et al., 2014).

The analysis of mass movement susceptibility became popular in recent decades with the development of GIS techniques (Carrara et al., 1991). Susceptibility maps show the likelihood of occurrence of certain natural hazardous phenomena in an area, while hazard maps quantify the probability of such occurrence. In general, the various methods used for the assessment of mass movement susceptibility can be divided into direct and indirect methods, and qualitative and quantitative methods (Holec et al., 2013). Quantitative methods such as the bivariate statistical method (Süzen & Doyuran 2004; Bednarik et al., 2010; Constantin et al., 2011), the multivariate statistical method (Clerici, 2002; Bednarik et al., 2005; Clerici et al., 2006), the frequency ratio method (Lee & Talib 2005), and the neural network method (Lee et al., 2003; Alkhasawneh et al., 2014; Aghdam et al., 2016) as well as methods using the fuzzy approach (Ercanoglu & Gokceoglu, 2002) are widely adopted and can be powerful tools for reducing risks caused by dangerous natural phenomena.

Several landslide susceptibility analyses were prepared for the territory of the Western Carpathians using multivariate and bivariate statistical analyses (Bednarik & Pauditš, 2010; Bednarik et al., 2010, 2012; Bednarik & Liščák 2010; Holec et al., 2013). Although a debris flow susceptibility analysis for the Western Carpathians has not been carried out yet, the geomorphological and dendrogeomorphological aspects of debris flows in this territory were studied by e.g., Šilhán & Pánek (2010).

Debris flow and shallow landslide susceptibility are more specific analyses in comparison with the assessment of more general mass movement susceptibility. Nevertheless, it has been topic of several studies involving various approaches such as the probabilistic approach (Chang et al., 2014), the modified certainty coefficient method (Wang et al., 2014), weights of evidence

Manuscript received 2017-10-01
Revised version accepted 2018-05-11

(Meyer et al., 2014), multivariate analysis (Baeza & Corominas, 2001; Santacana et al., 2003; Shen et al., 2012), logistic regression analyses (Can et al., 2005), and the analytic hierarchy process method (Chen et al., 2015; Xingzhang et al., 2015). Moreover, comparisons among various statistical and physically based models for debris flow susceptibility (Carrara et al., 2008) and among various pixel sizes in debris flow assessment (Cama et al., 2014) have been carried out.

The territory of Slovakia is influenced by the activity of various mass movements, and gravitational deformations cover about 5 % of the country's area (Kopecký et al., 2008). Only 4.3 % of mass movements in Slovakia are flows (Kopecký et al., 2008). Most flows are concentrated in the highest mountain ranges of the Western Carpathians, namely the Tatry Mountains, the Nízke Tatry Mountains, the Malá Fatra Mountains, the Veľká Fatra Mountains, and the Chočské vrchy Mountains (Nemčok et al., 1975). They are depicted in Fig. 1. The largest debris flow event in the last decade occurred in the Vrátna dolina locality, which is situated in the Malá Fatra Mountains. (Fig. 1). This area suffered considerable damage due to huge debris flows on 21 July 2014 caused by a rainfall anomaly (Šťastný et al., 2014). Fortunately, there were no fatalities; nevertheless, the event caused infrastructure damage – the lift station and the road to the village of Terchová were damaged. On the other hand, this event raised the interest of the public in hazardous geological, hydrological, and meteorological phenomena.

The main goal of this paper is to determine the debris flow susceptibility for the Krivánska Fatra Mountains, the most vulnerable part of the Malá Fatra Mountains, in order to learn more about the debris flow phenomena in the area. This assessment can help prevent the consequences of future events, and understand the importance of the main factors that cause debris flows. The bivariate and multivariate statistical methods were used to conduct susceptibility analyses. Two main susceptibility assessments were carried out: *(i)* in the first analysis the data from older debris flows were used; *(ii)* the second susceptibility assessment was carried out using older data as well as 2014 event data in order to create a new prognostic map. Various approaches were adopted to verify susceptibility analyses using the older debris flow map and data from the 2014 event. A comparison of two assessments using the differences of two susceptibility maps can be useful in attempting to assess hazards in the area.

2. REGIONAL SETTINGS

The prerequisite for the evolution of slope movements in the Malá Fatra Mountains is based on local geological and geomorphological conditions. There are several rock formations with low shear strength in the complex geological setting of the Malá Fatra Mountains. The important horizon are Lower Triassic red to variegated marly shales of the Tatric Unit and

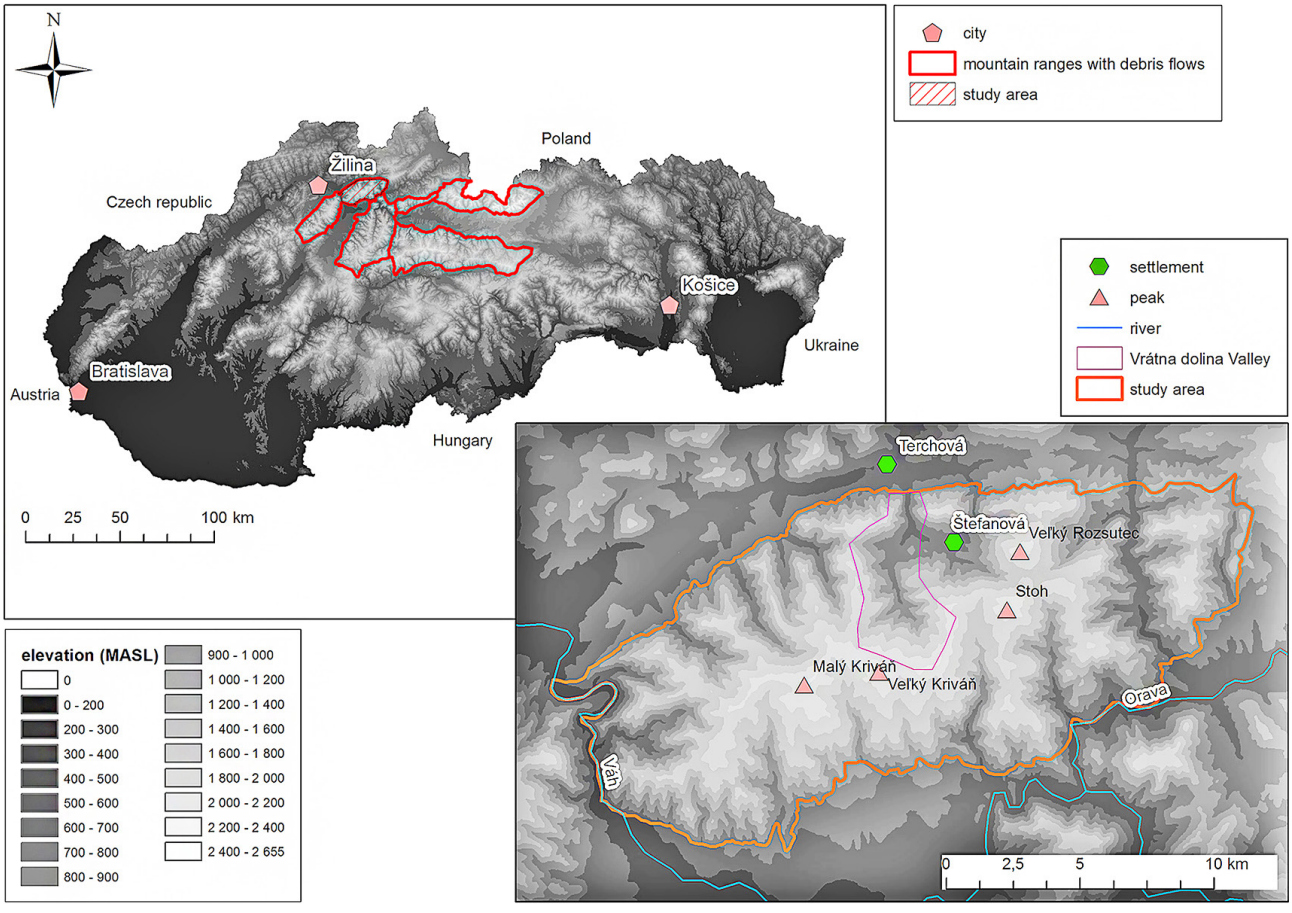

Fig. 1. Location of the study area.

Upper Triassic shales of the Carpathian Keuper Formation in the Fatric Unit. Mottled grey marly shales and marls are also found within Jurassic limestone formation and finally the highest members of the Lower Cretaceous grey marls and marly shales (Baliak et al., 1981).

Susceptibility to slope movement arises in the valleys where rapid progressive stream erosion exposes semisolid rocks overlain with solid rocks. The soft rock below the more resistant overlaying rocks are found on much steeper slopes and cannot sustain their natural inclination. An acute state of imbalance occurs when erosion exposes an interface of two different complexes. The same danger of imbalance exists wherever rapidly progressive erosion creates a slope that is steeper than the dip of the surfaces of discontinuities in the rock mass. Vast quantities of both of these cases can be found in the Malá Fatra Mountains.

The most frequent slope deformation processes in the Malá Fatra Mountains are creep movements (creeping), in the form of block movements or the disintegration of the mountain ranges. Shear zones present the schistose strata exposed in the lower part of the high steep slopes where plastic deformation occurs. Overburdened complexes are susceptible to fracture along predisposed surfaces with detached blocks at their periphery, and then slide down the subsoil and disintegrate slowly. The blocks usually consist of limestone and dolomite in the stratigraphic or tectonic superposition over the schistose strata of Early Triassic, Late Triassic, Early/Middle Jurassic and Early Cretaceous. In addition to the above block ridges and block fields within the Mesozoic complexes, the rock massifs and limestone-dolomite complexes are greatly disturbed by fault and fissure systems of different directions. On the surface, they are manifested in a step-wise morphology, such as ridges split into partial blocks (Baliak et al., 1981).

The disturbed balance is recovered in the less steep slopes made solely of soft argillaceous rocks. In the Werfen Fm., Carpathian Keuper Fm. or Albian rocks, the failure mechanism is similar to the processes in clay soils. The rocks, however, have somewhat higher strength characteristics, and the resulting shapes are slightly different. Sliding occurs on very steep and high slopes and is manifested in steps in the head scarps, while accumulation forms also remain in steep slopes. The shapes are often morphologically very clear and represent the mostly current active movements. On a slope formed by obliquely inclined strata, landslide movements occur over weakness planes and rockslides sometimes reach massive proportions.

Sudden movements of loose rubble induced by inrushes of water during storms arise within the erosion ravines with steep gradients. These mass movements of a flowing character often have disastrous consequences. Equally dangerous are sudden rockfalls of fragment blocks falling from high steep walls made of limestone and dolomite.

Typical debris flows are formed on steep slopes where superficial deposits have accumulated due to weathering and slope processes. Much of the material of debris flows originated from talus cones where the material accumulated in larger thicknesses. Stone runs begin above the forest line and often converge deep into valleys and destroy forest stands. They are composed of granitoids that are formed mainly on the southern slopes of the main ridge and are usually simple or branched, for instance on the slopes of Mount Veľký Fatranský Kriváň. Several stone runs have been identified on the slopes of Mount Stoh, Stienky, and Chleb, where rocky material is mixed with loamy slope debris.

Geomorphologically, the Krivánska Fatra is a subunit of the Malá Fatra Mountains belonging to the Inner Western Carpathians (Mazúr & Lukniš, 1978). The southern part called Lúčanská Fatra is divided by the antecedent gorge of the Váh River and is generally lower with a smaller occurrence of debris flows. The highest point of the Krivánska Fatra is 1709 m asl., while the lowest point, with an altitude of 350 m asl., is located in the Váh River gorge. This extreme altitude span within the small area of the Krivánska Malá Fatra results in a very high vertical dissection of surface – more than 640 meters in the central part of the range with a radius of 2.5 km using the method of Mazúr & Mazúrová (1965), and up to 1000 meters in certain parts. Steep slopes of up to 45° in the highest parts of main ridge are common. The geological structure is reflected in the land surface; dolomites and limestones of the Choč Nappe form blocks, which contrast with the smoothly modelled surfaces of marly limestones and shales of the Krížna Nappe (Lukniš & Plesník, 1961). The saddles are formed mainly by less resistant rocks, whilst the higher parts of the mountains are formed by more resistant rocks (Lukniš & Plesník, 1961). The uppermost parts of Vrátna dolina Valley are made of less resistant shales of the Mráznica Formation, which are overlain by limestones and dolomites resistant to erosion. This creates the steep slopes in the valley. The presence of glaciers during Quaternary was a matter of debate between geologists and geomorphologists (Nemčok, 1973) but it has yet to be proven. On the other hand, the evidence of Pleistocene periglacial and nival processes can be seen in present landscape of the area (Zaťko et al., 1983). Avalanches are common in the Krivánska Malá Fatra Mountains (Szalmová et al., 2013) and knowledge about them can be important for the research of debris flows, because the tracks of debris flows and avalanches are often the same. According to Szalmová et al. (2013), 99 avalanche tracks have been mapped in Krivánska Malá Fatra.

According to Bochníček et al. (2015), the main part of the territory is a cool mountainous sub-region with an average July temperature of less than 12 °C. The highest parts of the mountain range are cold mountainous sub-regions with an average July temperature of less than 10 °C (Alpine climate *E* according to Köppen classification). The Malá Fatra occupies a specific position among the first high Carpathian range, which is perpendicularly oriented toward prevailing winds. This fact causes increased rainfall and strong winds in comparison with similar mountains (Lukniš & Plesník, 1961). The average annual precipitation exceeds 1700 mm in the highest parts of mountain range and snow cover lasts for more than 5 months (Bochníček et al., 2015), which creates a significant water supply for potential debris flows in the area.

The forest area is dominated by beech forests. The spruce forest zone was partially reduced due to the lowering of the timberline for the herding purposes in the 17th century (Dobošová, 2002). The original altitude of the timberline, which was 1450 m asl. on average, is now 1200 m asl. on average. The cover was reduced strongly in the past and replaced by grasslands (Lukniš & Plesník,

1961; Zaťko et al., 1983). Nowadays, the pasture is still present in small parts of the study area but to a lesser degree. Planting of *Pinus mugo* started in the 1960s after reducing the pasture and declaration of preserved area in the Malá Fatra Mountains (Dobošová, 2002).

3. RECORDED CATASTROPHIC EVENTS IN THE STUDY AREA

Debris flows can be generated in the deep erosion ravines in the mouths of mountain valleys. In **1848,** the settlement of Štefanová was affected by a debris flow (in the chronicle described as a flood) which had catastrophic consequences (Pašek, 1975). Following a severe downpour on the night of June 11, 1848 in the Kreminná dolina Valley, a deep erosion ravine dissecting Veľký Rozsutec into Poludňové Skaly and Skalné mesto channelled the mighty debris flow. About 25 000 m^3 of slurry with boulders and broken tree trunks blocked the village, destroyed a major part of it and caused the death of 14 people (Pašek, 1975). A similar event, which was photo documented by Mr. Šaradín (Fig. 2), occurred in **1959** in the **Vrátna dolina Valley.**

The huge debris flows on **21 July 2014** were triggered in the **Vrátna dolina Valley** by a rainfall anomaly and caused considerable material losses. Before the event, the meteorological condition in Slovakia was influenced by two cyclonal situations with centres over northern Italy and the Baltic Sea (Šťastný et al., 2014). Because of flux convergence, sufficient humidity, high instability and convection, a line of slowly moving thunderstorms formed in northwestern Slovakia and moved from west to east. The area of the Malá Fatra Mountains was hit by two big waves of thunderstorms. The first wave began shortly after 3:00 p.m., and the second after 4:00 p.m. The total amount of precipitation during that day was 66 mm for the Vrátna station located in Štefanová, approximately 4 km from the event area. 52 mm of precipitation fell between 3:30 p.m. and 5:00 p.m. Data from 5 meteorological radar stations from Slovakia, the Czech Republic, and Poland showed that the Vrátna meteorological station was not in the epicentre of the thunderstorm. According to this data, there could have been approximately 90 millimetres of precipitation in the event area within an hour and 40 min (Šťastný et al., 2014).

Colluvial deposits are characterized by their large lithological variability depending on the basement rock. Loamy-stony and clayey slope sediments are developed on marly sediments of the Mráznica Fm. Debris flows were activated in these sediments below the ridge of about 1600–1500 m asl. (Fig. 3). The slope movements along the planar slip surface were conditioned by the favourable inclination of bedding. Within the detachment, areas of these landslides of rather small thickness quite small, but numerous "plates" of sliding material (with an area of several hundred m^2) broke away and generally moved at a speed of several meters per second, preferentially down avalanche chutes, often above extremely wet vegetation cover (grass, blueberries). Approximately 800 meters from the lower lift station of Vrátna, the thickness of the rolling mass of water-rock-earth-trees was measured on upright trees (Fig. 3). It seems that the thickness of the flow was up to 2 m – at the time of inspection (July 28, 2014), a creek of the depth of a mere 20 cm flowed there. A flow composed of water-clay-stones continued down the narrow valley. It also absorbed bottom fills which had accumulated in the previous period. Similar, although smaller debris flows from the tributaries joined it at different time depending upon their source distance. Most of them eroded valleys down to the bedrock. Two main debris flows joined (funnel-like confluence, Fig. 3) approximately 560 m from the cable car lower station. Moreover, a mobilization of rocky debris from the surrounding slopes contributed to the material of the debris flows. In these

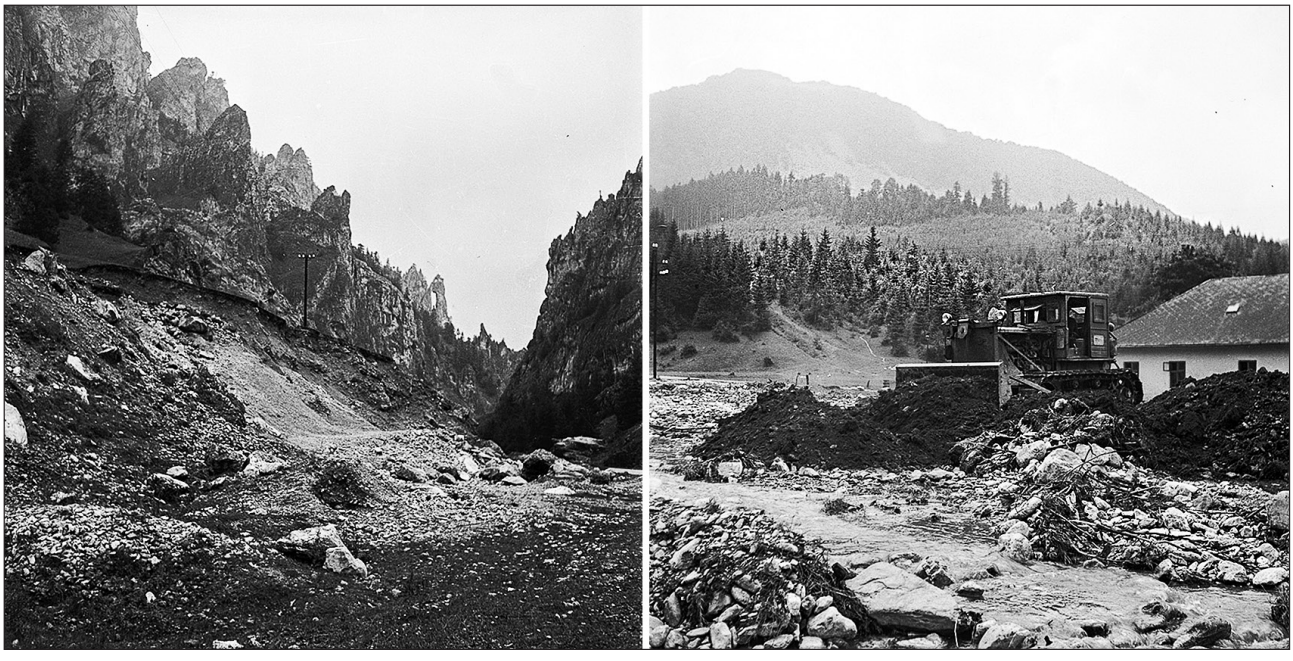

Fig. 2. Debris flow event in the Vrátna dolina Valley in 1959 (part Tiesňavy on the left, probably settlement Starý dvor on the right).

Fig. 3. Catastrophic debris flow in the Vrátna dolina Valley from July 2014: a) head scarps of debris flows below the main ridge in the part called Steny; b) accumulation part of the event near cottage Vrátna; c) buried valley cable line terminal at the toe of the event; d) cars hit by debris flow near the valley cable car terminal.

parts of the area, rock falls of fragments and blocks probably occurred. Many trees that remained standing registered fresh bark incisions, due to the impacts of fragments and blocks (at a height of up to 2 m above ground), which also contributed to the material of the debris flows. The total cubic capacity of the displaced material is estimated at a minimum of 100 000 m^3. The toe of the debris flow reached the cable line terminal, which experienced property damage, but without any serious static damage to buildings and lifts.

4. INPUT DATA AND METHODOLOGY

Unless stated otherwise, ArcGIS 10 was used for data processing. The following parametric maps were chosen to perform the susceptibility analysis: elevation, slope, plan curvature, flow accumulation, topographic wetness index (TWI), lithology, and land cover. Data on elevation, slope, plan curvature, flow accumulation, and TWI were calculated from a digital elevation model DMR 3.5 based on contours from the base map at a scale of 1:10 000. Pixel size of the model provided by Geodesy, Cartography and Cadastre Authority of Slovak Republic under contract No. 140-102-2768/2016 is 10 meters. The elevation map partially substituted the precipitation data. The elevation map was reclassified into 8 classes using the equal interval method (Fig. 5A). Slope steepness is a very important characteristic, which determines the energy of the processes on certain parts of the slope. The slope data were reclassified into 8 classes using the division used by Hrašna (1986) in engineering geological evaluations (Fig. 5B). The plan curvature marks the energy convergence or divergence. No exact value is determined in the literature to distinguish between convex, concave, and linear slopes. Some authors (e.g., Wang et al., 2014) use these 3 classes in susceptibility assessments; others (Cama et al., 2014) split the plan curvature into more classes. In this study, 3 classes of plan curvature representing the convexity, concavity, and linearity of the slope were used. A value of – 0.15 was used as the threshold between the concave and linear forms and a value of + 0.15 was used as the threshold between the linear and convex forms (Fig. 5C). Flow accumulation shows the accumulated weight of all cells flowing into each downslope cell in the output raster. This parameter was computed using the GRASS 7.0 (GRASS Development Team, 2017) *r.terraflow* module (Fig. 6B). The topographic wetness index (TWI) was used to assess the

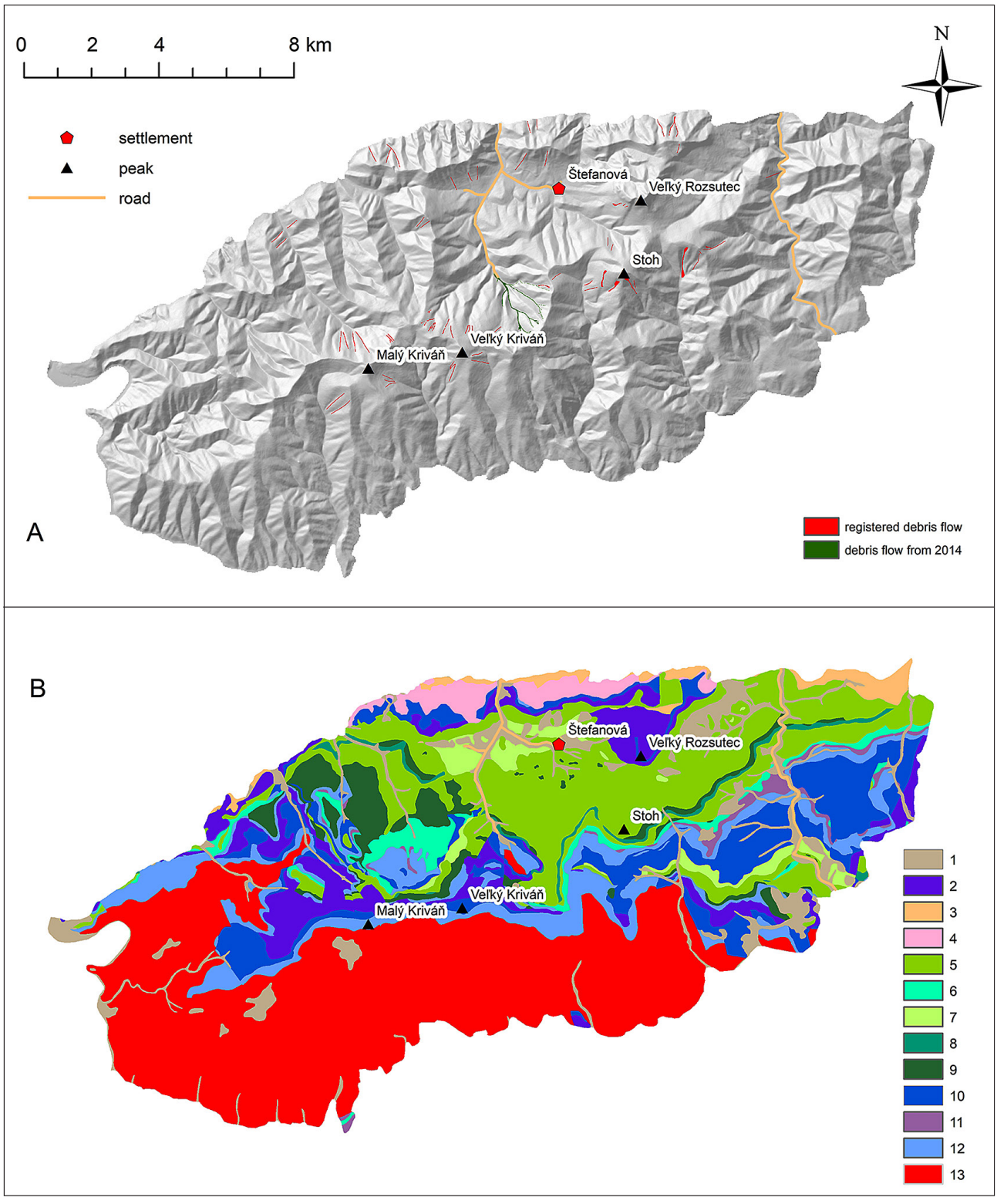

Fig. 4. Input parametric maps: a) registered debris flow events in various periods; b) lithological units (see legend in the Tab. 1).

potential of water infiltration volumes (Cama et al., 2014). Its value was computed as $TWI = A_s / ln\ tan\ \beta$, where A_s is the local upslope area obtained from flow accumulation and β is the slope steepness in degrees obtained from the slope raster (Fig. 6A). Lithological data were taken from the base geological map at a scale of 1:50 000 (Haško & Polák, 1978). The original map was simplified and 13 reclassified categories were used in the input parametric map (Fig. 4B). The data on land use were used from the Corine land cover database downloaded from the European Environmental Agency using the 3rd level of classification from the year 2012 (http://land.copernicus.eu/pan-european/corine-land-cover/clc-2012). Categories with negligible extent

were merged together, so that the input parametric map was reclassified into 11 categories (Fig. 6C). Data showing area of classes in input parametric maps are in Tabs. 1 and 2.

The input data about debris flows were taken from three time periods:

1) Debris flow events registered from the 1950s up to the 1970s (the first period data):

The map of Nemčok et al. (1975) at a scale of 1:25 000, which is focused on mass movements in the Malá Fatra Mountains was used as the primary source. The 60 debris flows in the Malá Fatra Mountains are depicted as line elements with a constant width of one pixel, i.e., 10 meters. The orthophotomap from 1950 taken from (http://mapy.tuzvo.sk/hofm/default.aspx) was used as secondary source to gain the areal representation of debris flows. The orthophotomap was created by processing the archival greyscale aerial photographs from the 1940s and 1950s from the Topographic Institute of the Slovak Republic. The resolution of the orthophotomap is 0.5 meter. We were able to adjust only 12 of the debris flows taken from Nemčok et al. (1975) to the orthophotomap from 1950 – in these cases the original line elements were converted into polygons. 10 debris flows identified in the orthophotomap were not depicted in map of Nemčok et al. (1975) and were added to the inputs.

2) Debris flow events registered from 2006 to 2010 (second period data):

The atlas of slope stability maps (Šimeková et al., 2006) and the orthophotomap from 2010 (http://mapy.tuzvo.sk/hofm/default.aspx) were taken, but contained only some of the debris flows from older sources and no new debris flows were discovered from these newer data.

3) Debris flow events registered in 2014 (third period data):

Finally, the layer of July 2014 catastrophic debris flows in the Vrátna dolina Valley from State Geological Institute of Dionýz Štúr was taken. The input map of debris flows is depicted in Fig. 4A.

4.1. BIVARIATE ANALYSIS

The bivariate analysis compares landslide map with each parametric map separately. Method has been widely used during last two decades (Süzen & Doyuran, 2004; Thiery et al., 2007; Yalcin, 2008; Bednarik et al., 2010; Nandi & Shakoor, 2010; Constantin et al., 2011; Holec et al., 2013). Secondary reclassification of input parametric maps based on debris flow density within each category was carried out. Weight of each input independent variable was calculated by method using entropy index proposed by Vlčko et al. (1980). The value of probability P_{ij} is expressed (Eq. 1), where p_{sd} represents the area covered by landslides within a given primarily reclassified category with area p_c. The density of probability (p_{ij}) is expressed as proportion of probability p_{ij} and the sum of probabilities within the whole parameter, s_j represents the number of classes within the parameter (Eq. 2).

The entropy index express the rate of disorderliness within parametric map, small entropy suggests relatively uniform density of landslides within each category of the parametric map, whilst big entropy shows unequal density of the landslides within parametric maps. Mathematically, the entropy Hj is expressed by (Eq. 3) and maximal entropy is expressed by (Eq. 4).

Ij is the information coefficient (Eq. 5) and the weight of parameter Wj is represented by (Eq. 6).

After this, the summation of weighted multiplication of secondary reclassified parametric maps is executed (Eq. 7), where W_j is the weight of the parameter, $sec\_parameter_j$ is the value of secondary reclassified category within given parameter, and m is the number of parameters.

Tab. 1. Reclassification of geological input parametric map.

Classes	Category description	Age	Area (km²)	Area (%)	biv_50_75	biv_50_75_14
1	Quaternary sediments	Quaternary	16.08	7.32	4	10
2	dolomites (Choč Nappe)	Mesozoic - Triassic	16.04	7.30	6	5
3	flysch sediments	Cenozoic - Palaeogene	3.5	1.59	10	6
4	main dolomites (Choč Nappe)	Mesozoic - Triassic	4.46	2.03	5	3
5	marly limestones, marls, shales (Krížna Nappe)	Mesozoic - Jurassic	40.11	18.25	9	11
6	shales, sandstones, limestones (Krížna Nappe)	Mesozoic - Jurassic	5.48	2.49	12	12
7	sandstones, calcareous sandstones, limestones with shales (Krížna Nappe)	Mesozoic - Cretaceous	4.47	2.03	11	8
8	radiolarites, radiolaric limestones (Krížna Nappe)	Mesozoic - Jurassic	2.14	0.97	13	13
9	marly limestones, sandy-encrinite limestones, grey muddy limestones (Krížna Nappe)	Mesozoic - Jurassic	9.28	4.22	8	9
10	Gutenstein limestones (Krížna and Choč Nappes)	Mesozoic - Triassic	22.29	10.14	2	4
11	organodetritic, coral and lumachelle limestones	Mesozoic - Triassic	2	0.91	3	2
12	sandstones, quartz sandstones and shales (Krížna Nappe)	Mesozoic - Triassic	19.16	8.72	7	7
13	granites and granodiorites - crystalline complex (Tatric Unit)	Palaeozoic (Devonian - Carboniferous)	74.72	34.01	1	1
Total			219.73	100.00		

biv_50_75: Categories of secondary reclassified parametric map using bivariate analysis from older data

biv_50_75_14: Categories of secondary reclassified parametric map using bivariate analysis from older data and 2014 event as well

Tab. 2. Reclassification of input parametric maps.

Elevation	Altitude interval (MASL)	Area (km²)	Area (%)	biv_50_75	biv_50_75_14
1	less than 400	1.49	0.68	1	1
2	400 - 600	18.08	8.23	2	2
3	600 - 800	64.99	29.58	4	3
4	800 - 1000	61.5	27.99	5	4
5	1000 - 1200	41.56	18.91	6	5
6	1200 - 1400	21.96	9.99	7	7
7	1400 - 1600	9.64	4.39	8	8
8	1600 - 1709	0.51	0.23	3	6
Total		219.73	100.00		
Slope angle	**Interval (°)**	**Area (km²)**	**Area (%)**	**biv_50_75**	**biv_50_75_14**
1	0 - 1	0.2	0.09	1	1
2	1 - 3	0.89	0.41	1	2
3	3 - 7	2.55	1.16	3	4
4	7 - 12	6.99	3.18	4	7
5	12 - 17	14.51	6.60	5	3
6	17 - 25	49.53	22.54	7	5
7	25 - 35	109.13	49.67	6	6
8	35 and more	35.93	16.35	8	8
Total		219.73	100.00		
Plan curvature	**Interval**	**Area (km²)**	**Area (%)**	**biv_50_75**	**biv_50_75_14**
1	less than -0.15 (concave)	69.02	31.41	3	3
2	-0.15 - 0.15 (quasi linear)	67.94	30.92	2	2
3	0.15 and more (convex)	82.77	37.67	1	1
Total		219.73	100.00		
TWI	**Interval (°)**	**Area (km²)**	**Area (%)**	**biv_50_75**	**biv_50_75_14**
1	2.11 - 4.85	48.79	22.20	1	1
2	4.85 - 5.49	56.36	25.65	2	2
3	5.49 - 6.38	60.81	27.67	3	3
4	6.38 - 22.64	53.77	24.47	4	4
Total		219.73	100.00		
Flow accumulation	**Interval (grid cells 10*10 m)**	**Area (km²)**	**Area (%)**	**biv_50_75**	**biv_50_75_14**
1	0 - 20	134.61	61.26	1	1
2	20 - 40	44.28	20.15	2	2
3	40 - 60	12.84	5.84	3	3
4	60 - 80	5.72	2.60	4	4
5	80 - 100	3.31	1.51	5	5
6	100 - more	18.97	8.63	6	6
Total		219.73	100.00		
Land Cover	**Category**	**Area (km²)**	**Area (%)**	**biv_50_75**	**biv_50_75_14**
1	Artificial surfaces and water area	0.45	0.20	1	1
2	Sport and leisure facilities	1.31	0.60	1	1
3	Broad-leaved forest	90.6	41.23	8	8
4	Coniferous forest	21.03	9.57	7	6
5	Mixed forest	76.62	34.87	6	7
6	Natural grasslands	13.19	6.00	11	11
7	Moors and heathland	5.06	2.30	9	9
8	Transitional woodland-shrub	2.67	1.22	1	1
9	Sparsely vegetated areas	0.51	0.23	10	10
10	Pastures	4.83	2.20	5	5
11	Arable land and heterogenous agricultural areas	3.46	1.57	1	1
Total		219.73	100.00		

biv_50_75: Categories of secondary reclassified parametric map using bivariate analysis from older data

biv_50_75_14: Categories of secondary reclassified parametric map using bivariate analysis from older data and 2014 event as well

The interval of susceptibility values using bivariate analysis was reclassified into five classes using method of natural breaks. The debris flow susceptibility was described as very low, low, moderate, high, and very high.

4.2. MULTIVARIATE ANALYSIS

Multivariate statistical analysis is based on a combination of all input parametric maps (lithology, slope, altitude, and slope deformations) and the subsequent application of information from areas where no event has been mapped. In the case of the conditional analysis (Clerici, 2002), the outcome is a table containing the topical combination of all input parametric maps, including all category combinations arising from the superposition of all of the input maps. These combinations make up new area elements, so-called unique conditional units (UCU), in the final map. No secondary reclassification or parameter weighting is needed prior to the multivariate analysis. The final combinations containing debris flow events (value 1, true in the map) are ordered based on the calculated occurrence intensity – the ratio of the landslide UCU cell number and UCU total area; the descending result gives the least favourable combinations (Clerici, 2002; Bednarik et al., 2005).

The UCU were computed in ArcGIS 10 software. The value ranges between 0 (no debris flow within UCU type) and 1 (the entire area of UCU type is covered by

Tab. 3. UCU with densities of debris flows higher than 70 %.

Multivariate analysis from first period data									
Elevation	Slope angle	Plan curvature	Flow accumulation	TWI	Geology	Land cover	Count(pixels)	Area (m^2)	Density of debris flows (%)
5	6	3	6	4	3	5	1	100	100.00
6	8	1	3	3	5	9	1	100	100.00
8	8	1	3	3	8	6	1	100	100.00
8	8	1	3	4	8	6	7	700	100.00
8	8	1	4	4	8	6	2	200	100.00
7	5	3	3	4	6	6	2	200	100.00
8	7	1	4	4	10	3	1	100	100.00
8	7	1	3	4	10	3	1	100	100.00
8	6	3	1	3	10	3	1	100	100.00
6	7	3	6	4	2	3	2	200	100.00
8	7	1	1	1	5	4	1	100	100.00
4	7	2	6	4	8	3	4	400	75.00
5	4	3	6	4	12	3	4	400	75.00
5	8	3	3	3	12	3	4	400	75.00
6	7	2	3	3	5	9	7	700	71.43

Multivariate analysis from first and third period data									
Elevation	Slope angle	Plan curvature	Flow accumulation	TWI	Geology	Land cover	Count(pixels)	Area (m^2)	Density of debris flows (%)
5	6	3	6	4	3	5	1	100	100.00
6	8	1	3	3	5	9	1	100	100.00
4	3	3	2	4	1	5	2	200	100.00
8	8	1	3	3	8	6	1	100	100.00
8	8	1	3	4	8	6	7	700	100.00
8	8	1	4	4	8	6	2	200	100.00
5	5	1	3	4	10	3	1	100	100.00
7	5	3	3	4	6	6	2	200	100.00
5	4	2	6	4	1	5	9	900	100.00
5	4	3	6	4	1	5	4	400	100.00
5	4	3	3	4	1	5	1	100	100.00
5	5	3	3	4	12	5	2	200	100.00
5	5	3	6	4	12	5	5	500	100.00
5	8	1	2	4	12	5	1	100	100.00
5	5	2	3	4	12	5	1	100	100.00
6	7	2	5	4	10	5	1	100	100.00
6	5	1	6	4	10	5	3	300	100.00
8	7	1	4	4	10	3	1	100	100.00
8	7	1	3	4	10	3	1	100	100.00
8	6	3	1	3	10	3	1	100	100.00
6	7	3	6	4	2	3	2	200	100.00
8	7	1	1	1	5	4	1	100	100.00
8	8	1	1	1	1	6	2	200	100.00
5	5	3	2	4	12	5	5	500	80.00
8	8	1	2	3	8	6	21	2100	76.19
4	7	2	6	4	8	3	4	400	75.00
5	4	3	6	4	12	3	4	400	75.00
5	8	3	3	3	12	3	4	400	75.00
8	7	3	2	3	1	6	4	400	75.00
4	4	3	6	4	1	5	38	3800	73.68
8	8	1	1	2	8	6	15	1500	73.33
6	7	2	3	3	5	9	7	700	71.43

Tab. 4. Results of simple raster overlaying analysis for various periods.

A - multivariate analysis		
Multivariate analysis 1st period vs. debris flows 1st period		
susceptibility class	pixels with debris flows	%
1 - very low	20	0.466
2 - low	43	1.003
3 - moderate	40	0.933
4 - high	52	1.212
5 - very high	4134	96.386
Multivariate analysis 1st period vs. debris flows 1st period+3rd period		
susceptibility class	pixels with debris flows	%
1 - very low	1242	20.341
2 - low	51	0.835
3 - moderate	78	1.277
4 - high	53	0.868
5 - very high	4682	76.679
Multivariate analysis 1st+3rd period vs. debris flows 1st period+3rd period		
susceptibility class	pixels with debris flows	%
1 - very low	43	0.704
2 - low	68	1.114
3 - moderate	85	1.392
4 - high	110	1.802
5 - very high	5800	94.989

B - bivariate analysis		
Bivariate analysis 1st period vs. debris flows 1st period		
susceptibility class	pixels with debris flows	%
1 - very low	0	0.000
2 - low	28	0.653
3 - moderate	432	10.072
4 - high	1914	44.626
5 - very high	1915	44.649
Bivariate analysis 1st period vs. debris flows 1st period+3rd period		
susceptibility class	pixels with debris flows	%
1 - very low	0	0.000
2 - low	99	1.621
3 - moderate	1059	17.344
4 - high	2137	34.998
5 - very high	2811	46.037
Bivariate analysis 1st+3rd period vs. debris flows 1st period+3rd period		
susceptibility class	pixels with debris flows	%
1 - very low	0	0.000
2 - low	69	1.130
3 - moderate	843	13.806
4 - high	2337	38.274
5 - very high	2857	46.790

debris flows). Small UCU of one or few pixels can be produced by positional inaccuracy of the inputs, on the other hand ratio of small UCU comparing to the study area is relatively low and does not influence the analysis results significantly. The results of multivariate analyses are usually reclassified into three or five conventional classes representing the level of susceptibility. The reclassification according to Clerici (2002) was applied in order to produce a debris flow susceptibility map. Five classes of susceptibility were created using the equation IR = 0.4 × MD; where IR is the interval range and MD is the mean density. Mean density was calculated as ratio of number of pixels with debris flows to number of pixels of the whole study area. The intervals

Tab. 5: Simple raster overlaying of multivariate analysis with avalanche tracks

Multivariate analysis 1st+3rd period vs. avalanche tracks			
susceptibility class			
1 - very low	51347	0,584	58,3979710210859
2 - low	1070	0,012	1,21693242044446
3 - moderate	1356	0,015	1,54220594590906
4 - high	1097	0,012	1,24764006096035
5 - very high	33056	0,376	37,5952505516002
Multivariate analysis 1st period vs. avalanche tracks			
susceptibility class			
1 - very low	47523	0,540	54,0488592680208
2 - low	1139	0,013	1,29540750176285
3 - moderate	1555	0,018	1,76853262971135
4 - high	1999	0,023	2,27350271819485
5 - very high	35710	0,406	40,6136978823101

0 – IR; IR – 2 × IR; 2 × R – 3 × IR; 3 × IR – 4 × IR; 4 × IR and more were chosen. The debris flow susceptibility was described as in previous case (very low, low, moderate, high, and very high).

Two main susceptibility maps were created for each method:

In the first map only the first time period data on debris flows were taken into account. This susceptibility map was verified by the dataset from the first time period and by a combination of the first time period with the third time period dataset.

The second susceptibility map covers data from the first and third time periods. It was verified by a combination of the first time period with the third time period dataset.

Various approaches to verify the results of conditional analyses were adopted in this study. The first approach involved the simplest method of verifying the prediction maps, namely a raster overlap of the registered deformation maps with the prediction maps (Bednarik, 2001, 2007, Nandi & Shakoor, 2010, Constantin et al., 2011).

Secondly, one of the most widely used methods for the evaluation of the model accuracy the Receiver Operator Characteristics (ROC) curves (Frattini et al., 2010) was adopted in the verification process. The size of the area under curve (AUC) defines the overall quality of the prediction model; the larger the area, the more successful the model. The ideal model has a maximum value of 1, whilst a trivial model has a value of AUC 0.5, which means a 50% success rate. The ROC curves are constructed using the contingency tables and their number corresponds to the threshold values. Subsequently, the true and false positive values (TP and FP) are calculated for each contingency value. Those values then define the shape of ROC curves.

Thirdly, the dataset of avalanche tracks was used to verify debris flow susceptibility results. ROC curve was also constructed to compare debris flow susceptibility with avalanche tracks.

5. RESULTS AND VERIFICATION PROCESS

5.1. Multivariate analysis

5.1.1. Assessment of debris flow susceptibility using events registered from the 1950s to the 1970s

The debris flow susceptibility map using a multivariate conditional analysis is shown in Fig. 7A. The results of multivariate analysis show the highest values concentrated around the main ridge. The most prone combinations of input parameters to debris flows are listed in the Tab. 3 Ten UCU are totally covered by debris flows and another four have a coverage of more than 70 %. The source area of catastrophic debris flows in the year 2014 is classified mainly in the highest category of susceptibility, whilst the transport and accumulation zones are in the lowest category of susceptibility. This fact supports the exceptionality of the 2014 event, whose magnitude is higher than any of the older debris flows mapped from older sources mapped from 1950s to 1970s and whose frequency is much lower than in the case of other debris flows.

5.1.2. Assessment of debris flow susceptibility using events registered from the 1950s to the 1970s and debris flow events registered in 2014

The debris flow susceptibility map using a multivariate conditional analysis based on older and 2014 events is shown in Fig. 7B. Twenty-three UCU are totally covered by debris flows and another nine have a coverage of more than 70% (Tab. 3). The results of the analysis show certain differences – the area from the 2014 event is categorised in higher categories of susceptibility. Similar areas in the other parts of the Malá Fatra Mountains are categorised in the high categories of susceptibility and show the possibility of future extreme debris flows. The Kreminná dolina Valley is one of the areas with increased susceptibility after the second evaluation. It was affected by a catastrophic debris flow in 1848 (Pašek, 1975), which destroyed the part of

Tab. 6: Comparison of both multivariate analyses and the relationship between the frequency and magnitude of debris flow events; the traffic light system shows the possible magnitude of the events and frequency rising from top to bottom

Assessment of debris flow susceptibility using events registered in 1950s till 1970s and debris flow events registered in 2014						
	susceptibility category	**very low (1)**	**low (2)**	**moderate (3)**	**high (4)**	**very high (5)**
Assessment of debris flow susceptibility using events registered in 1950s till 1970s	very low (1)	1883362	8954	7160	2425	30642
	low (2)	14640	20280		775	659
	moderate (3)		13712	2662	1714	2501
	high (4)			17978	1669	
	very high (5)			3777	22627	161724

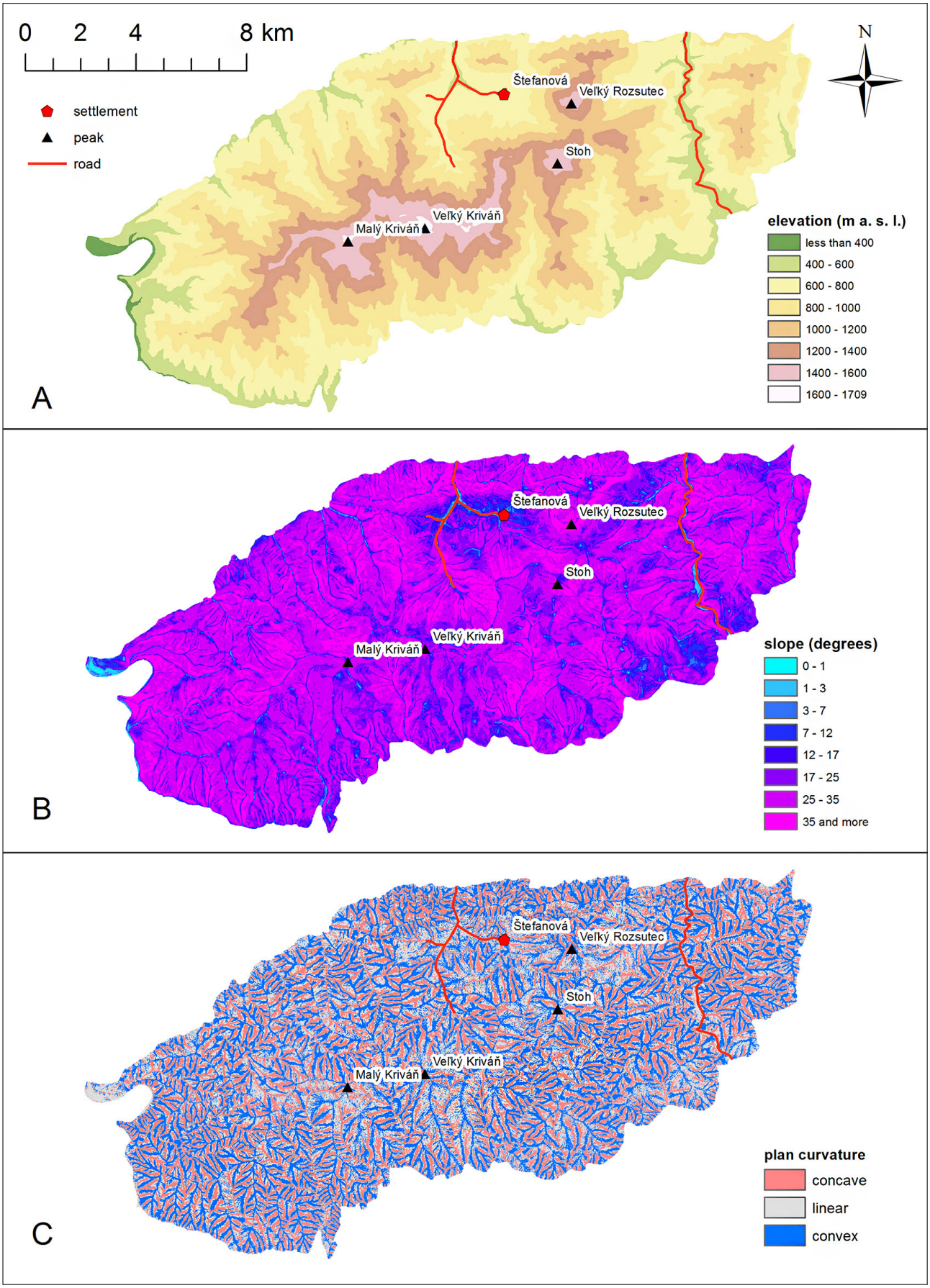

Fig. 5. Input parametric maps: a) digital elevation model; b) slope angle; c) plan curvature.

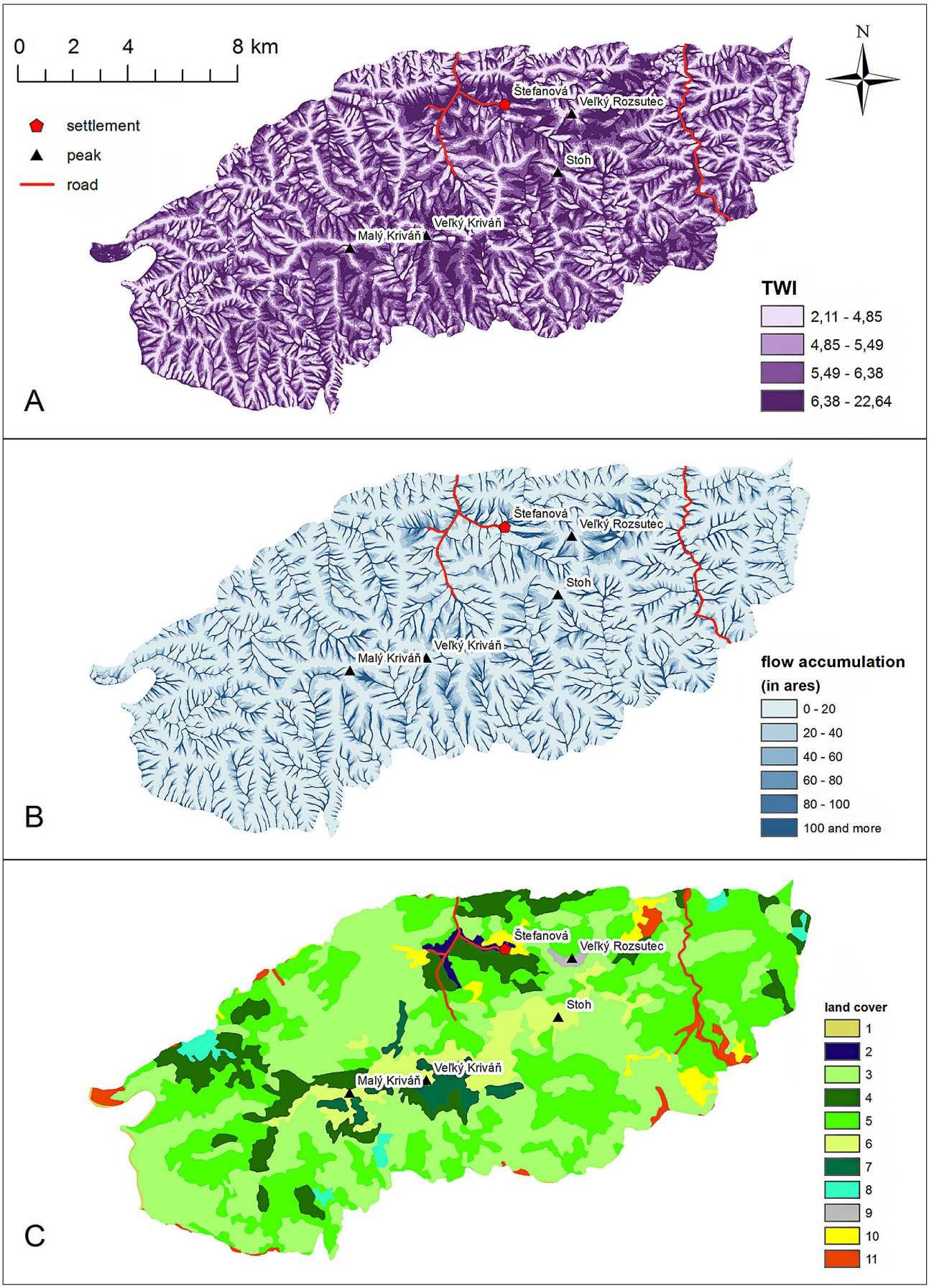

Fig. 6. Input parametric maps: a) topographic wetness index; b) flow accumulation; c) land cover (see legend in the Tab. 2).

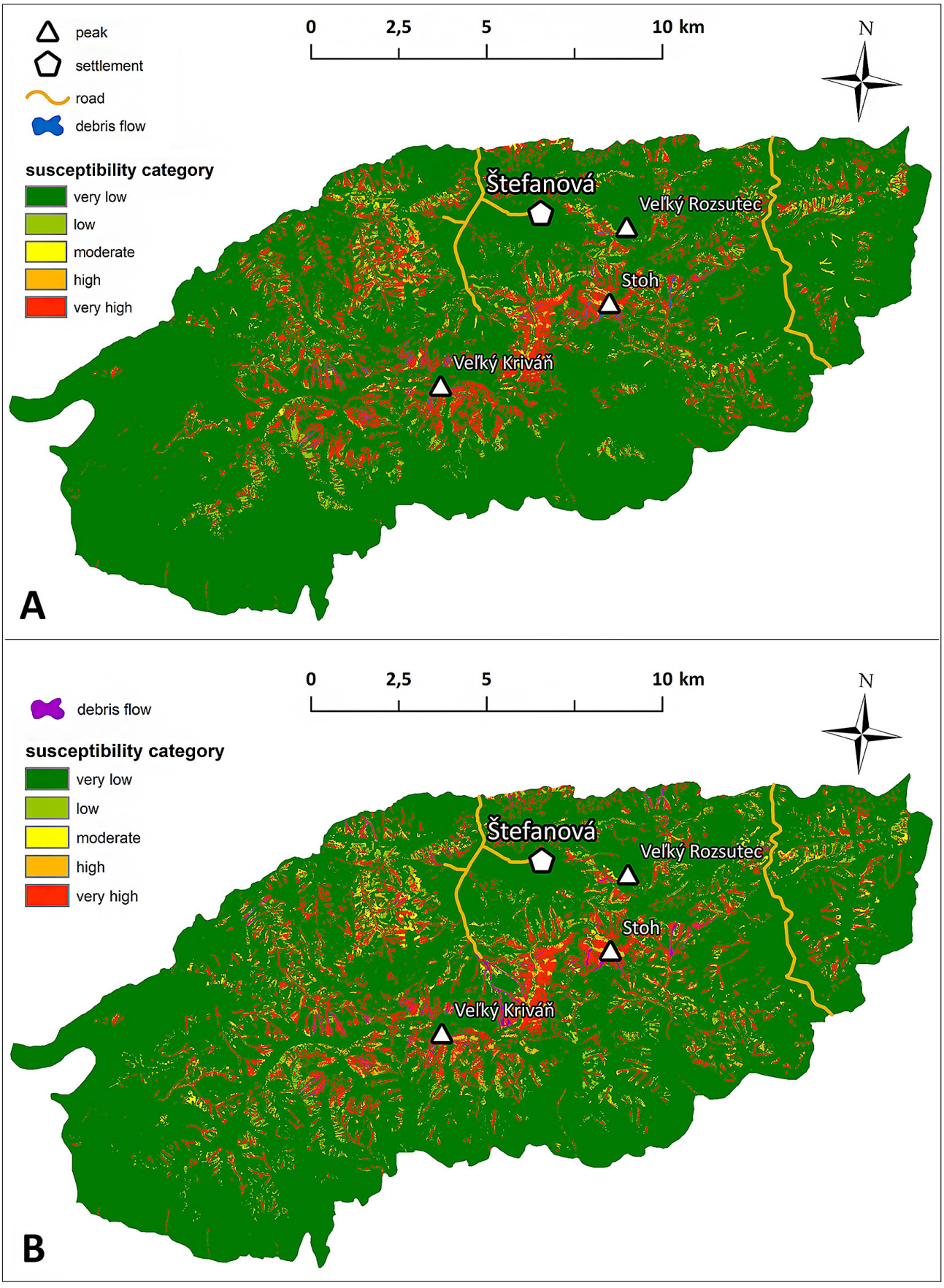

Fig. 7. Susceptibility maps using multivariate statistical analysis: a) assessment of debris flow susceptibility using events registered from the 1950s to the 1970s; b) assessment of debris flow susceptibility using events registered from the 1950s to the 1970s and debris flow events registered in 2014.

the settlement of Štefanová and caused serious casualties. The increased susceptibility of this area supports the reliability of the evaluation.

5.2. Bivariate analysis

5.2.1. Assessment of debris flow susceptibility using events registered from the 1950s to the 1970s

Following equation of bivariate analysis was computed from the secondary reclassified parametric maps:

susceptibility = 0.00162 × landcover + 0.00114 × elevation + 0,00063 × TWI + 0,00052 × lithology + 0.00044 × plan curvature + 0.00038 × slope + 0.00035 × flow accumulation

Secondary reclassification of input parameters is shown in Tabs. 1 and 2. Parameters of land cover and elevation show relatively high weight in comparison with other parameters, approximately two times higher than the third most important parameter. This fact is caused by intensive occurrence of debris flows in the areas of main ridge – the biggest probability density is in the classes of DEM between 1200 and 1600 m asl. and in the land cover classes natural grasslands and sparsely vegetated areas. It causes high level of susceptibility in the whole central area of the Malá Fatra Mts. (Fig. 8A). Parameter of slope shows surprisingly low weight, the reason can be found in the using of whole debris flow for the analysis, not only their upper (erosion) part.

5.2.2. Assessment of debris flow susceptibility using events registered from the 1950s to the 1970s and debris flow events registered in 2014

The equation of bivariate analysis using the 2014 events as well is following:

susceptibility = 0,0022 × landcover + 0,0015 × elevation + 0,00101 × TWI + 0,0008 × plan curvature + 0,00077 × lithology + 0,00068 × flow accumulation + 0,00022 × slope

Order of first three parameters is the same as in previous equation, plan curvature changed its position with lithology and flow accumulation with slope. Susceptibility map is depicted in Fig. 8B.

5.2.3. Various approaches of verification debris flow susceptibility maps

Herein, various approaches of debris flow susceptibility verification are presented. It has to be noted that the used verification can be divided into two cases: in the first case the dataset used for creation of the susceptibility map was the same as the dataset used for verification, e.g. susceptibility computed from older events was verified by these older data. Several authors applied the simplest way of verification – overlying of mass movements map by susceptibility map (e.g., Bednarik, 2001, 2007; Nandi & Shakoor, 2010; Constantin et al., 2011). The second case was when the dataset used for creation of susceptibility map was verified by updated dataset (e.g., susceptibility computed from older events was verified by the older and new data – events from 1950s to the 1970s and events from 2014 as well.) or another independent dataset (avalanche tracks). It is then logically explainable that the verifications from the second case are showing generally lower accuracy rates.

1) Verification using simple raster overlaying

The fastest and simplest method for verifying results was the raster overlaying of a prognostic map with debris flow inventory maps.

The results of multivariate analysis show a high correspondence between the results of the susceptibility analysis and existing debris flows (Tab. 4A). Using the category of very high debris flow susceptibility, the verification of the debris flow susceptibility map using events registered from the 1950s to the 1970s by this older data has an accuracy rate of 96.4 %. The verification of the debris flow susceptibility map using events registered from the 1950s to the 1970s by this older data and debris flow events registered in 2014 has an accuracy rate of 76.7 %. The verification of the debris flow susceptibility map using events registered from the 1950s to the 1970s and events registered in 2014 by this older data and debris flow events registered in 2014 has an accuracy rate of 95 %.

In the case of bivariate analysis the correspondence is lower in comparison with multivariate analysis (Tab. 4B). The percentage of debris flows within very high susceptibility class varies between 44 % and 47 %. If two highest susceptibility classes are taken into account (high and very high susceptibility), the accuracy fluctuates between 80 % and 90 %.

2) ROC curves

The results of ROC curves as proof for susceptibility assessment are shown in Fig. 9. The verification of the debris flow susceptibility map from multivariate analysis using events registered from the 1950s to the 1970s by this older data has an accuracy rate of 95.3 %. The verification of the debris flow susceptibility map using events registered from the 1950s to the 1970s by this older data and debris flow events registered in 2014 has an accuracy rate of 85.12 %. The verification of the debris flow susceptibility map using events registered from the 1950s to the 1970s and events registered in 2014 by this older data and debris flow events registered in 2014 has an accuracy rate of 95.03 %.

ROC curves used for bivariate analysis assessment indicate lower, but more balanced accuracy rates between 79 % and 83 %.

3) Verification using the dataset of avalanche tracks

A comparison of existing avalanche tracks and debris flow susceptibility based on multivariate analysis was carried out taking into account the morphological difference between a debris flow track and an avalanche track. The first has a more linear shape, whilst the second is broader in its upper part. As a result, many avalanche tracks contain areas with high debris flow susceptibility but low to high susceptibility in their broader upper part. The value of AUC comparing avalanche tracks and the results of the debris flow susceptibility assessment from older data and 2014 debris flows was 67.6 %. The extent of avalanche tracks corresponds well with the mapped susceptibility in the area of catastrophic debris flows from 2014. Simple raster overlaying of multivariate analysis with avalanche tracks shows lesser correspondence between the results of the susceptibility analysis and existing avalanche tracks (Tab. 5).

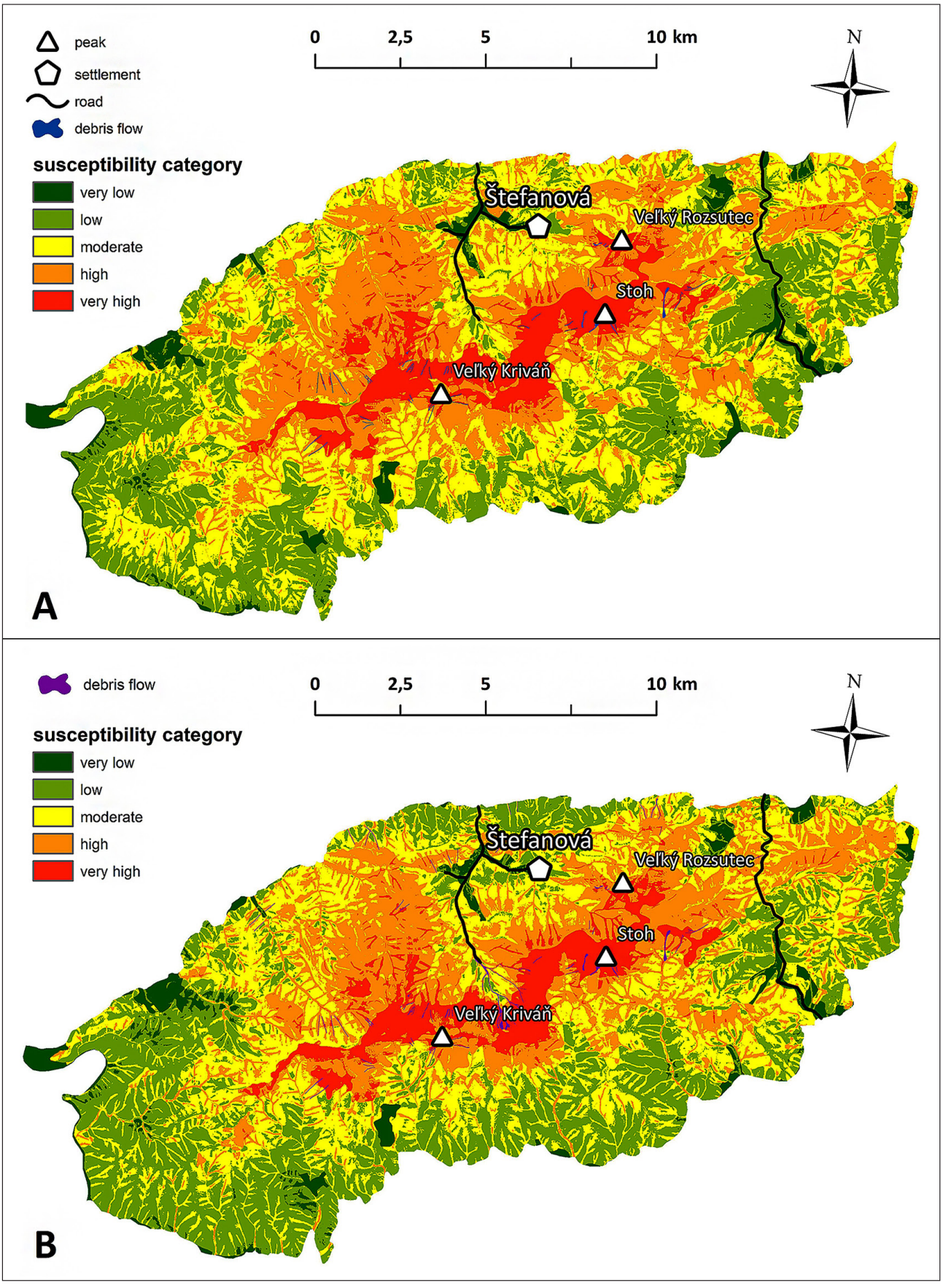

Fig. 8. Susceptibility maps using bivariate statistical analysis: a) assessment of debris flow susceptibility using events registered from the 1950s to the 1970s, b) assessment of debris flow susceptibility using events registered from the 1950s to the 1970s and debris flow events registered in 2014.

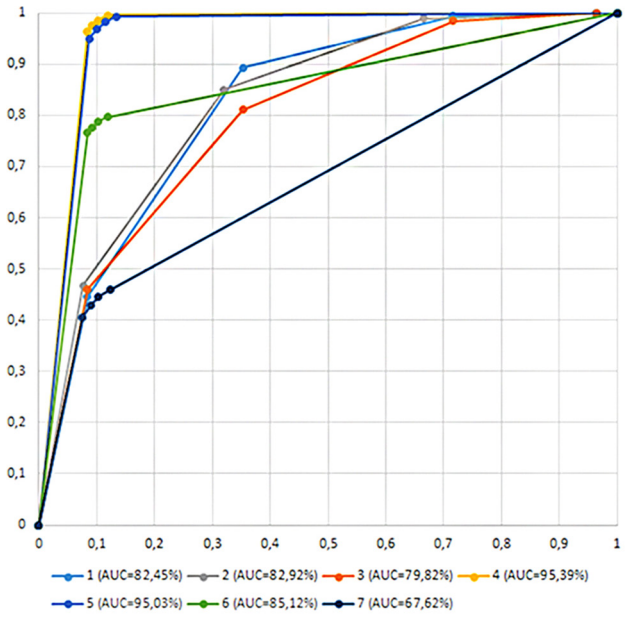

Fig. 9. ROC curves and AUC results, false positive rate on x axis, true positive rate on y axis; 1) bivariate susceptibility assessment from the first period vs. data from the first period; 2) bivariate susceptibility assessment from the first and third periods vs. data from the first and third periods; 3) bivariate susceptibility assessment from the first period vs. data from the first and third periods; 4) multivariate susceptibility assessment from the first period vs. data from the first period; 5) multivariate susceptibility assessment from the first and third periods vs. data from the first and third periods; 6) multivariate susceptibility assessment from the first period vs. data from the first and third periods; 7) multivariate susceptibility assessment from the first data period vs. data from avalanche tracks.

6. DISCUSSION

By combining the results of two multivariate analyses (Fig. 7A,B) the experimental evaluation of debris flow hazard in the area can be assessed. The main idea is that the data from first analysis (Fig. 7A) shows the susceptibility to high frequency – low magnitude events. On the other hand, the second map is constructed using the data of debris flows registered from the 1950s to the 1970s and the extraordinary 2014 low frequency-high magnitude event. According to the studied map sources from the 1950s to 1970s and from 2006 to 2010, they do not show such extraordinary debris flows as those from 2014. The last recorded extraordinary debris flow in the area took place in 1848 (Pašek, 1975). However, there is no exact map of this event, just the information about its range which was comparable with event from 2014. Due to lack of older data, the frequency of these events can be assessed only indirectly and it can be stated that their recurrence frequency is more than 65 years, in the order of hundreds of years. The difference between the two results of multivariate analyses (Fig. 7A,B) can indicate susceptibility to low frequency – high magnitude events. Tab. 6 shows the results of combining the two analyses in the form of a matrix. Columns show the susceptibility using data of debris flows registered from the 1950s to the 1970s and the extraordinary 2014 low frequency – high magnitude event (Fig. 7B), rows show the susceptibility created only from high frequency – low magnitude events (Fig. 7A). Number of pixels is shown within certain category of susceptibility. The upper right corner marked in deep orange colour shows that there are 30 642 pixels (i.e. areas) which belong to lowest class of susceptibility

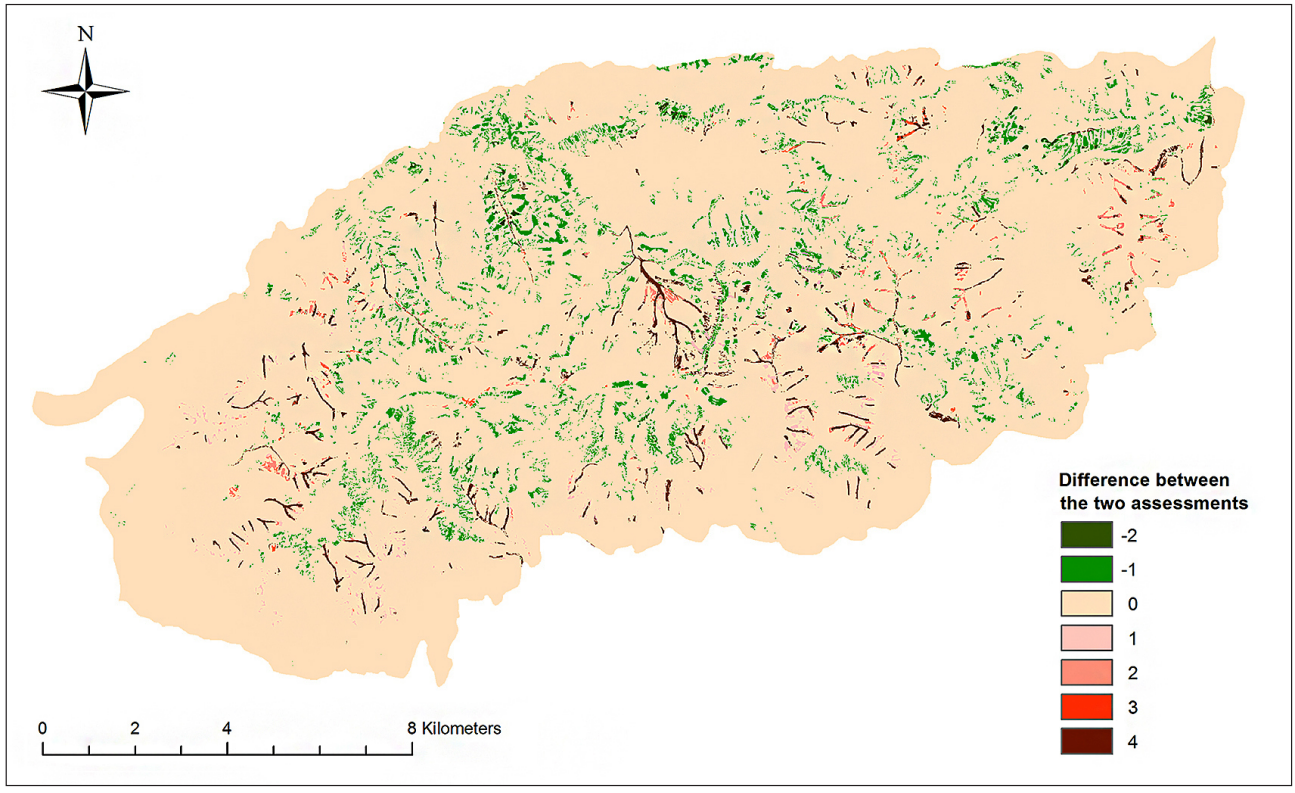

Fig. 10. Differences map of multivariate analyses (subtraction of first period data assessment from first and third period data assessment).

in the analysis in Fig. 7A, but to the highest class in the analysis in Fig. 7B, so they indicate high possibility of low frequency-high magnitude events. The diagonal of the table indicates the categories without change in susceptibility between the two analyses. On the contrary, the categories in the lower left part marked in green colours indicate the prevalence of hazards caused by high frequency – low magnitude phenomena; thus, the assessment using the 1950s–1970s and 2014 data showed a lower class of susceptibility. The debris flow recurrence possibility increases from the top row to the bottom row, and the possibility of extreme events increases from the bottom row to the top row in the table. The map presenting the differences between the two multivariate analyses created as the difference between Fig. 7B and Fig.7A is depicted in Fig. 10. Herein the highest values marked in deep red colour indicate the biggest possibility of low frequency – high magnitude events.

7. CONCLUSIONS

The multivariate analysis has been used and verified by three various methods which show a very good prediction value of the model. However, the bivariate analysis shows less reliable results if the verification from the raster overlaying and ROC curve are taken into account. The verification using the ROC curve in the case of the multivariate analysis with AUC (area under curve) shows results of more than 95 %, whilst a value of approximately 83 % is shown for the bivariate analysis. Thus, the multivariate analysis is the more suitable of these two methods for the assessment of debris flow susceptibility. This could be due to the specific quasi-linear shape of debris flows. Using the multivariate analysis, very small units (UCU) are created, and thus the assessment can be spatially more accurate. Using the bivariate analysis, the larger areas are affected by a certain type of susceptibility and the weighting process gives a certain weight to a larger area connected to a certain category of the input parametric map. In the case of this study, the land cover input had the largest weight with the natural grasslands as the category with the highest density of debris flows; thus, the majority of the main ridge of the Malá Fatra Mountains was set in the highest category of susceptibility using the bivariate analysis. In conclusion, the accuracy for such small, quasi linear entities like debris flows was limited by this method.

Despite of sufficient results from bivariate analysis, the multivariate analysis is more adequate for this study. Its reliability has been proven by three various methods of verification showing good (comparing with avalanche tracks) to excellent results (using raster overlaying and ROC curves). The existence of catastrophic debris flows from July 2014 which damaged local infrastructure is a specific feature of the area. It served to verify the results of multivariate analyses carried out with data from the 1950s to the 1970s. The extraordinary nature of the event was proven by comparison with older registered events and the susceptibility map from older registered events. A new susceptibility map including the 2014 event was constructed. The results of the two maps can serve as an experimental as a tool to outline sites with increased debris flow hazard in the study area. However, it has to be noted that no exact recurrence interval can be assessed.

Acknowledgments: This work was partially supported by Comenius University in Bratislava under contract No. UK/228/2016, by the Slovak Research and Development Agency under contract No. APVV-0129-12, No. APVV-16-0146 and by the Scientific Grant Agency of the Ministry of Education, Science, Research and Sport of the Slovak Republic and the Slovak Academy of Sciences (VEGA) within the projects No. 1/0602/16 and No. 1/0131/14. Authors would like to thank to Pavel Šťastný from Slovak Hydrometeorological Institute for providing the information and data about meteorological situation preceding the catastrophic debris flows in July 2014 and to Lucia Szalmová from Slovak Environment Agency for providing the data about avalanche tracks from the area.

References

Aghdam I.N., Varzandeh M.H.M. & Pradhan B., 2016: Landslide susceptibility mapping using an ensemble statistical index (Wi) and adaptive neuro-fuzzy inference system (ANFIS) model at Alborz Mountains (Iran). *Environmental Earth Sciences*, 75, 553–573.

Alexander D., 2004: Natural hazards on an unquiet earth. *In:* Matthews J. & Herbert D. (Eds.): Unifying geography. Common heritage, shared future. Routledge, London, pp. 266–282.

Alkhasawneh M.S., Ngah U.K., Tay L.T. & Isa N.A.M., 2014: Determination of importance for comprehensive topographic factors on landslide hazard mapping using artificial neural network. *Environmental Earth Sciences*, 72, 3, 787–799.

Baeza C. & Corominas J., 2001: Assessment of shallow landslide susceptibility by means of multivariate statistical techniques. *Earth Surface Processes and Landforms*, 26, 1251–1263.

Baliak F., Nemčok A. & Pašek J., 1981: Slope deformations in the Krivánska Malá Fatra Mts. [Svahové deformácie v Krivánskej Malej Fatre]. *In:* Janík M. & Štollmann A. (Eds.): Rozsutec. Štátna prírodná rezervácia. Vydavateľstvo Osveta, pp. 126–142.

Bednarik M., 2001: Susceptibility assessment of Handlovská kotlina basin for mass movements [Hodnotenie náchylnosti územia Handlovskej kotliny na svahové pohyby]. Master thesis, Prírodovedecká fakulta Univerzity Komenského, Bratislava, 40 p.

Bednarik M., 2007: Landslide risk assessment for the purposes of spatial planning documentation [Hodnotenie zosuvného rizika pre potreby územnoplánovacej dokumentácie]. Dissertation thesis, Prírodovedecká fakulta Univerzity Komenského, Bratislava, 130 p.

Bednarik M. & Liščák P., 2010: Landslide susceptibility assessment in Slovakia. *Mineralia Slovaca*, 42, 193–204.

Bednarik M. & Pauditš P., 2010: Different ways of landslide geometry interpretation in a process of statistical landslide susceptibility and hazard assessment : Horná Súča (western Slovakia) case study. *Environmental Earth Sciences*, 61, 733–739.

Bednarik M., Clerici A., Tellini C. & Vescovi P., 2005: Using GIS GRASS in evaluation of landslide susceptibility in Termina valley in the Northern Appennines (Italy). *In:* Moser M. (Ed.) Proceedings of the Conference on Engineering Geology: Forum for young engineering geologists. DGGT Erlangen-Nürnberg, Fridrich-Alexander-University of Erlangen-Nürnberg, April 6th to 9th 2005, pp. 19–24.

Bednarik M., Magulová B., Matys M. & Marschalko M., 2010: Landslide susceptibility assessment of the Kraľovany–Liptovský Mikuláš railway case study. *Physics and Chemistry of the Earth*, 35, 162–171.

Bednarik M., Yilmaz I. & Marschalko M., 2012: Landslide hazard and risk assessment: a case study from the Hlohovec–Sereďlandslide area in southwest Slovakia. *Natural Hazards*, 64, 547–575.

Bochníček O., Borsányi P., Čepčeková E., Faško P., Chmelík M., Jančovičová Ľ., Kapolková H., Labudová L., Mikulová K., Mišaga O., Nejedlík P., Pribullová A., Snopková Z., Šťastný P., Švec M. & Turňa M., 2015: Climate atlas of Slovakia [Klimatický atlas Slovenska]. Slovenský hydrometeorologický ústav, Bratislava, 131 p.

Cama M., Conoscenti C., Lombardo L. & Rotigliano E., 2014: Exploring relationships between pixel size and accuracy for debris flow susceptibility models: a test in the Giampilieri catchment (Sicily, Italy). *Environmental Earth Sciences*, 75, 238–258.

Can T., Nefeslioglu H.A., Gokceolu C., Sonmez H. & Duman T.Y., 2005: Susceptibility assessments of shallow earthflows triggered by heavy rainfall at three catchments by logistic regression analyses. *Geomorphology*, 72, 250–271.

Carrara A., Cardinali M., Detti R., Guzzetti F., Pasqui V. & Reichenbach P., 1991: GIS techniques and statistical models in evaluating landslide hazard. *Earth Surface Processes and Landforms*, 16, 5, 427–445.

Carrara A., Crosta G. & Frattini P., 2008: Comparing models of debris-flow susceptibility in the alpine environment. *Geomorphology*, 94, 353–378.

Chang M., Tang C., Zhang D. & Ma G., 2014: Debris flow susceptibility assessment using a probabilistic approach: A case study in the Longchi area, Sichuan province, China. *Journal of Mountain Science*, 11, 1001–1014.

Chen H.X., Zhang S., Peng M. & Zhang L.M., 2015: A physically-based multihazard risk assessment platform for regional rainfall-induced slope failures and debris flows. *Engineering Geology*, 203, 15–29

Clerici A., 2002: A GRASS GIS based shell script for landlide susceptibility zonation by the conditional analysis method. *In:* Ciolli M. & Zatelli P. (Eds.): Proceedings of the Open source GIS GRASS users conference, Trento, Italy, 1–17.

Clerici A., Perego S., Tellini C. & Vescovi P., 2006: A GIS-based automated procedure for landslide susceptibility mapping by the Conditional Analysis method: The Baganza valley case study (Italian Northern Apennines). *Environmental Geology*, 50, 941–961.

Constantin M., Bednarik M., Jurchescu M.C. & Vlaicu M., 2011: The landslide susceptibility assessment using the bivariate statistical analysis and the index of entropy in the Sibiciu Basin (Romania). *Environmental Earth Sciences*, 63, 397–406.

Dobošová A., 2002: Sub-alpine meadows of National Park Malá Fatra. What is their future from the botanist´s point of view? [Hole Národného parku Malá Fatra, aká je budúcnosť z pohľadu botanika]. *Oecologia Montana*, 11, 35–37.

Ercanoglu M. & Gokceoglu A.E.C., 2002: Assessment of landslide susceptibility for a landslide-prone area (north of Yenice, NW Turkey) by fuzzy approach. *Environmental Geology*, 41, 720–730.

Frattini P., Crosta G. & Carrara A., 2010: Techniques for evaluating the performance of landslide susceptibility models. *Engineering Geology*, 111, 62–72.

GRASS Development Team, 2017: Geographic Resources Analysis Support System (GRASS) Software, Version 7.4. Open Source Geospatial Foundation. Electronic document: http://grass.osgeo.org

Haško J. & Polák M., 1978: Geological map of the Kysucké vrchy and Krivánska Malá Fatra Mountains, 1:50 000. State geological Institute of Dionýz Štúr, Bratislava.

Holec J., Bednarik M., Šabo M., Minár J., Yilmaz I. & Marschalko M., 2013: A small-scale landslide susceptibility assessment for the territory of Western Carpathians. *Natural Hazards*, 69, 1081–1107.

Hrašna M., 1986: Maps of engineering geological districts for the urbanization purposes [Mapy inžinierskogeologického rajónovania pre účely urbanizácie]. *In: Zborník referátov z vedeckej konferencie Progresívne smery v inžinierskogeologickom výskume*. PRIF UK Bratislava, Katedra inžinierskej geológie, pp. 68–82.

Kopecký M., Ondrášik M., Martinčeková T. & Šimeková J., 2008: Landslide Atlas [Atlas zosuvov]. *Enviromagazín*, 5, 8–9.

Lee S. & Talib J.A., 2005: Probabilistic landslide susceptibility and factor effect analysis. *Environmental Geology*, 47, 982–990.

Lee S., Ryu J.H., Lee M.J. & Won J.S., 2003: Use of an artificial neural network for analysis of the susceptibility to landslides at Boun, Korea. *Environmental Geology*, 44, 820–833.

Lukniš M. & Plesník P., 1961: Lowlands, basins and mountains of Slovakia [Nížiny, kotliny a pohoria Slovenska]. Osveta, Bratislava.

Mazúr E. & Lukniš M., 1978: Regional geomorphologic division of Slovak socialist republic. [Regionálne geomorfologické členenie Slovenskej socialistickej republiky]. *Geografický časopis*, 30, 2, 101–125.

Mazúr E. & Mazúrová V., 1965: Map of relative vertical ruggedness and its possibility for creating geographical districts. [Mapa relatívnej výškovej členitosti Slovenska a možnosti jej použitia pre geografickú rajonizáciu]. *Geografický časopis*, 17, 1, 3–18.

Meyer N.K., Schwanghart W., Korup O., Romstad B. & Etzelmüller B., 2014: Estimating the topographic predictability of debris flows. *Geomorphology*, 207, 114–125.

Nandi A. & Shakoor A., 2010: A GIS-based landslide susceptibility evaluation using bivariate and multivariate statistical analyses. *Engineering Geology*, 110, 1–2, 11–20.

Nemčok A., 1973: Genesis of Chleb kettles and its importance for creating the objects of Directive spatial plan in Vrátna dolina Valley [Genéza chlebských kotlov a jej význam pre uskutočnenie objektov Smerného územného plánu vo Vrátnej]. Geofond, Bratislava.

Nemčok A., Baliak F., Mahr T. & Malgot J., 1975: Systematic research of slope deformations in Slovakia [Systematický výskum svahových deformácií na Slovensku]. Štátna výskumná úloha II.-8-7/8. Katedra geotechniky stavebnej fakulty v Bratislave, Bratislava.

Pašek J., 1975: Mythic Mount Rozsutec [Bájna hora Rozsutec]. *Lidé a země*, 24, 3, 116–119.

Santacana N., Baeza B., Corominas J., de Paz A. & Marturía J., 2003: A GIS-Based Multivariate Statistical Analysis for Shallow Landslide Susceptibility Mapping in La Pobla de Lillet Area (Eastern Pyrenees, Spain). *Natural Hazards*, 30, 281–295.

Shen C.W., Lo W.C. & Chen C.Y., 2012: Evaluating Susceptibility of Debris Flow Hazard using Multivariate Statistical Analysis in Hualien County. *Disaster Advances*, 5, 4, 743–755

Smith K & Petley D. N,, 2009. Environmental hazards: assesing risk and reducing disaster. Routledge, New York. 383 pp.

Süzen M.L. & Doyuran V., 2004: Data driven bivariate landslide susceptibility assessment using geographical information systems: a method and application to Asarsuyu catchment, Turkey. *Engineering Geology*, 71, 303–321.

Szalmová L., Minár J. & Žiak M., 2013: Regional typification and selection of representative avalanche paths in Malá Fatra Mts. *Acta Geographica Universitatis Comenianae*, 57, 1, 17–30.

Šilhán K. & Pánek T., 2010: Dynamics of Debris Flows in the Culmination Parts of the Moravskoslezské Beskydy Mts. *Studia Geomorphologica Carpatho-Balcanica*, 44, 49–61.

Šimeková J., Martinčeková T., Abrahám P., Gejdoš T., Grenčíková A., Grman D., Hrašna M., Jadroň D., Záthurecký A., Kotrčková E., Liščák P., Malgot J., Masný M., Mokrá M., Petro Ľ., Polaščinová E., Solčiansky R., Kopecký M., Žabková E. & Wanieková D., 2006. Atlas of slope stability maps of the Slovak Republic (1:50 000). [Atlas máp stability svahov (1:50000)] Žilina: Ingeo.

Šťastný P., Turňa M., Méri L. & Zaujec P.,2014. Meteorological evaluation of storm activity in the area of northwestern Slovakia. [Meteorologické zhodnotenie búrkovej činnosti na severozápadnom Slovensku 21. júla 2014]. Vodohospodársky spravodajca, 57, 24–25.

Takahashi T., 2014. Debris flow. Mechanics, prediction and Countermeasures. Taylor and Francis Group, London. 551 pp.

Thiery Y., Malet J-P., Sterlacchini S., Puissant A. & Maquaire O., 2007: Landslide susceptibility assessment by bivariate methods at large scales: Application to a complex mountainous environment. *Geomorphology*, 92, 38–59.

Vlčko J., Wagner P. & Rychlíková Z., 1980: Evaluation of regional slope stability. *Mineralia Slovaca*, 12, 3, 275–283.

Wang J., Yu Y., Yang S., Lu G. & Ou G., 2014: A modified certainty coefficient method (M-CF) for debris flow susceptibility assessment: A case study for the Wenchuan earthquake meizoseismal areas. *Journal of Mountain Science*, 11, 1286–1297.

Xingzhang C., Hui C., Yong Y. & Jinfeng L., 2015: Susceptibility assessment of debris flows using the analytic hierarchy process method. A case study in Subao river valley, China. *Journal of Rock Mechanics and Geotechnical Engineering*, 7, 4, 404–410.

Yalcin A., 2008: GIS-based landslide susceptibility mapping using analytical hierarchy process and bivariate statistics in Ardesen (Turkey): Comparisons of results and confirmations. *Catena*, 72, 1, 1–12.

Zaťko M., Lukniš M., Plesník P., Mládek J., Seko L., Škvarček A., Zatkalík F., Bizubová M., Korec P., Slavík V., Spišiak P. & Zaťková M.,1983: Physical-geographical characteristization of geomorphological units in Slovakia. [Fyzickogeografická charakteristika geomorfologických celkov Slovenska]. Report. Prírodovedecká fakulta UK, Bratislava.

Web:

http://mapy.tuzvo.sk/hofm/default.aspx

http://land.copernicus.eu/pan-european/corine-land-cover/clc-2012